ARTICLE

Controlled Copolymerization of *n*-Butyl Acrylate with Semifluorinated Acrylates by RAFT Polymerization

Senbin Chen[a] and Wolfgang H. Binder*[a]

Reversible Addition Fragmentation chain Transfer (RAFT) copolymerization of *n*-butyl acrylate (*n*BuA) with semifluorinated acrylates, such as 2,2,2-trifluoroethyl acrylate (TFEA), 2,2,3,3,3-pentafluoropropyl acrylate (PFPA) and 2,2,3,3,4,4,4-heptafluorobutyl acrylate (HFBA) up to 90.2% co-monomers conversion was accomplished. When using dibenzyl trithiocarbonate (DBTTC) as chain transfer agent (CTA) in DMF at 65 $^{\circ}$C, excellent control of molecular weight (Mn) together with a low molecular weight distribution (PDI) was achieved. The successful synthesis of well-controlled semifluorinated copolymers was checked by a combination of ^{1}H NMR, ^{19}F NMR, SEC and ESI-TOF mass spectrometry, proving their composition via ^{1}H NMR and ESI-TOF mass spectrometry. The reactivity ratios (r) of each pair of co-monomers were assessed by Fineman-Ross (FR) and Kelen-Tüdos (KT) laws: in all cases, the product ($r_{M1} \times r_{M2}$) was close to unity, indicating a random distribution of each pair of co-monomers along the semifluorinated copolymers backbone. Results were further confirmed by applying the *Q-e* scheme.

Introduction

Benefitting from the presence of strong and highly polar carbon-fluorine bond, it is well known that fluorine containing polymers exhibit many remarkable intrinsic properties, such as excellent resistance to chemicals, heat, UV-radiation, as well as display valuable electrical properties, low adhesive forces and a low surface energy. Therefore, fluorine containing materials have various promising applications, and are current topics of active research.[1-10]
There has been a growing realization of synthetic (semi)fluorinated polymers and materials in both fundamental and applied research over the last couple of decades, relying on a multitude of polymerization techniques (such as polycondensation,[11] living anionic,[12-17] living cationic,[18] conventional radical[19-22] or living radical polymerization, atom transfer radical polymerization (ATRP),[23-29] single-electron transfer living radical polymerization (SET-LRP),[30] nitroxide-mediated radical polymerization (NMP)[31], reversible addition-fragmentation chain transfer (RAFT) or Macromolecular Design via the Interchange of Xanthates (MADIX) polymerization[32-36] techniques). Especially the formation of semicrystalline polymers is often an important characteristic of many homofluoropolymers,[37-39] together with their high chemical resistance. Thus copolymerization is often employed to adjust the properties of manufactured polymers to meet specific needs, such as improved solubility and modified surface properties. As a result, the generation of fluorinated copolymers which do not exhibit the limit of homopolymers mentioned above, has attracted considerable attention recently.[9]
Thus for example, Ameduri and co-workers have investigated conventional radical copolymerization of semifluorinated

acrylates with morpholinoethyl methacrylate[40] and acrylonitrile,[41] in detail studying the reactivity ratios of each co-monomers. By copolymerizing vinylidene fluoride with a synthesized 2-trifluoromethacrylate monomer containing a C_6F_{13}-side chain (monomer: 3,3,4,4,5,5,6,6,7,7,8,8,8-tridecafluorooctyl 2-(trifluoromethyl)acrylate) the superior thermostability and hydrophobicity of the obtained copolymers were demonstrated by the same group[42] very recently, initiating the first radical copolymerization of chlorotrifluoroethylene and 3,3,4,4-tetrafluoro-4-bromobut-1-ene with *tert*-butylperoxypivalate.[43] Urban and co-workers[44] presented the conventional radical copolymerization of methyl methacrylate and *n*BuA monomers with a wide range of semifluorinated monomers, i.e., 3,3,4,4,5,5,6,6,7,7,8,8,9,9,10,10,10-heptadecafluorodecyl methacrylate, 3,3,4,4,5,5,6,6,7,7,8,8,9,9,10,10,10-heptadecafluorodecyl acrylate; 3,3,4,4,5,5,6,6,7,7,8,8,9,9,10,10,10-heptadecafluoro-1-decene; 2,2,3,3,4,4,4-heptafluorobutyl acrylate; and 2,2,3,3,4,4,4-heptafluorobutyl methacrylate, which resulted in the generation of stable colloidal dispersions that carry up to 8.5% (w/w) of F-containing copolymers. In addition, 2-methylene-1,3-dioxepane was copolymerized with several fluoroalkenes ($R_fCH=CH_2$) using azobis(isobutyronitrile) (AIBN) as initiator: ^{1}H NMR spectroscopy proved that all the obtained polymers were effectively alternating copolymers of caprolactone and fluoroalkene.[45]
Compared to conventional radical polymerization, the formation of (semi)fluorinated copolymers relying on controlled radical polymerizations (mainly ATRP,[46] NMP and RAFT/MADIX[36, 47-53] still remains limited, although among these controlled radical polymerizations, RAFT/MADIX polymerization has been known as one of the most versatile

methods for providing structurally well-controlled macromolecules.[54] Destarac and co-workers[49] have reported the RAFT/MADIX copolymerization of vinyl trifluoroacetate with vinyl acetate or vinyl pivalate using a xanthate chain transfer agent (O-ethyl-S-(1-methoxycarbonyl)ethyl dithiocarbonate) also employing vinyl trifluoroacetate as a vinyl acetate co-monomers in the RAFT/MADIX process in order to increase the solubility of poly(vinyl esters) in supercritical CO_2.[50] Bai and co-workers[51] demonstrated the RAFT copolymerization of chlorotrifluoroethene with butyl vinyl ether under [60]Co γ-ray irradiation using S-benzyl O-ethyl dithiocarbonate as chain transfer agent, obtaining well-defined alternating copolymers. Recently, the same group reported the xanthate-mediated living radical copolymerization of hexafluoropropylene with butyl vinyl ether, generating fluorinated copolymers with well-defined molecular weight and narrow molecular weight distribution.[52]

Aiming at an improved solubility as well as further potential application on surfaces in this context we wish to report the copolymerization of n-butyl acrylate (nBuA) with a range of semifluorinated acrylates, e.g. 2,2,2-trifluoroethyl acrylate (TFEA), 2,2,3,3,3-pentafluoropropyl acrylate (PFPA) and 2,2,3,3,4,4,4-heptafluorobutyl acrylate (HFBA) in DMF at 65 °C, using dibenzyl trithiocarbonate (DBTTC) as chain transfer agent, to afford well-controlled poly(nBuA-co-TFEA), poly(nBuA-co-PFPA) and poly(nBuA-co-HFBA) (see **Scheme 1**). Moreover, we have studied the obtained copolymer compositions in detail via mass spectrometric techniques, and further evaluated the reactivity ratios of each pair of co-monomers via Fineman-Ross and Kelen-Tüdos laws, to assess the distribution of both co-monomers along the copolymers backbone.
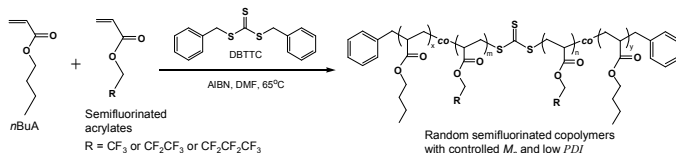
Scheme 1: Synthetic route to random semifluorinated copolymers, mediated by DBTTC in DMF at 65 °C.

Experimental part

Materials

All the chemicals were purchased from Alfa Aesar or Sigma-Aldrich. nBuA was filtered prior to passing through a column of basic aluminium oxide to remove inhibitors. All the semifluorinated acrylates, TFEA, PFPA and HFBA, were purified by vacuum distillation. 2,2'-Azobis(isobutyronitrile) (AIBN) was recrystallized twice from ethanol. DBTTC was synthesized according to a previous report.[55] Unless otherwise indicated the other chemicals were used without further purification.

Characterization methods

^{1}H and ^{13}C NMR spectra were recorded on a Varian Gemini 2000 FT-NMR spectrometer (400 MHz) or a Varian unity Inova 500 (500 MHz) NMR spectrometer using $CDCl_3$, CD_2Cl_2 or THF-d_8 as solvents.

(Co)polymers were analysed by size exclusion chromatography (SEC), running in THF at 35°C (flow rate: 1 mL·min^{-1}) and recorded on a GPCmax VE 2001 from Viscotek™, equipped with a column set of a H$_{HR}$-H Guard-17369 column, a CLM30111 column and a G2500H$_{HR}$-17354 column. The number-average molecular weight of all the (co)polymers was derived from a calibration curve based on polystyrene.

ESI-TOF MS measurements were carried out on a Bruker Daltonics micrOTOF time-of-flight ESI-MS system. Spectra were recorded in the positive or negative-ion mode (accelerating voltage = 4.5kV, desolvation temperature = 180 °C, scan range = 50 - 15000 m/z) subsequently processed on a Bruker Daltonics ESI compass 1.3 for the micrOTOF (Data Analysis 4.0). Polymers were dissolved in methanol (MeOH) (10 g/L) and injected into the ESI-ion source by a micro-syringe pump (injection speed of 300 μL/min).

Homopolymerization of HFBA

Solution homopolymerization of HFBA was carried out using DBTTC as RAFT agent and AIBN as initiator. Typically, solution polymerization of HFBA (1.79 mL, 1.0×10^{-2} mol) was carried out using AIBN (1.64 mg, 1.0×10^{-5} mol), DBTTC (29.0 mg, 1.0×10^{-4} mol) and DMF (2.0 mL) as solvent, also acting as an internal reference for the measurement of HFBA consumption via ^{1}H NMR. A stock solution was typically transferred into a flask sealed with a rubber septum, deoxygenated by nitrogen bubbling for ~30 min at 0 °C, then immersed into an oil bath thermostatted at 65 °C. The reaction was stopped by plunging the flask into liquid nitrogen. The polymer was subsequently precipitated twice into MeOH/H_2O (1/1, v/v) in order to eliminate residual monomer. The polymer was dried under vacuum and characterized by ^{1}H NMR, ^{19}F NMR and SEC. The molar mass of pure PHFBA was finally evaluated by ^{1}H NMR (THF-d_8) from the relative integration of the characteristic ester group protons of the PHFBA backbone (-O-CH_2-CF$_2$-, 2nH, δ = 4.68 ppm, with n being the degree of polymerization) and the characteristic aromatic protons of DBTTC (ph$H$, 10H, δ = 7.12-7.30 ppm).

Copolymerization of nBuA with HFBA

Solution copolymerization of nBuA with HFBA was carried out using DBTTC as RAFT agent, and AIBN as initiator. Typically, solution copolymerization of nBuA (0.35 mL, 2.5×10^{-3} mol) with HFBA (0.5 mL, 2.5×10^{-3} mol) was carried out using AIBN (1.64 mg, 1.0×10^{-5} mol), DBTTC (29 mg, 1.0×10^{-4} mol) and DMF (0.5 mL) as solvent, also acting as an internal reference for the measurement of nBuA and HFBA consumption via ^{1}H NMR. A stock solution was typically transferred into a flask sealed with rubber septum, deoxygenated by nitrogen bubbling for ~30 min at 0 °C, then immersed in an oil bath thermostatted at 65 °C. The reaction was stopped by plunging the flask into liquid nitrogen. The

copolymer was subsequently precipitated twice into MeOH/H$_2$O (1/1, v/v) in order to eliminate residual *n*BuA and HFBA, dried under vacuum and characterized by ^{1}H NMR, ^{19}F NMR, SEC and ESI-TOF mass spectrometry. The molar mass of pure poly(*n*BuA-*co*-HFBA) was finally evaluated by ^{1}H NMR (CD$_2$Cl$_2$) via relative integration of the characteristic ester group protons of the P*n*BuA backbone (-O-C*H$_2$*-CH$_2$-, 2mH, δ = 4.05 ppm, with m being the degree of polymerization), the PHFBA backbone (-O-C*H$_2$*-CF$_2$-, 2nH, δ = 4.61 ppm, with n being the degree of polymerization) and of the characteristic aromatic protons of DBTTC (ph*H*, 10H, δ = 7.13-7.37 ppm).

Copolymerization of *n*BuA with PFPA

Solution copolymerization of *n*BuA with PFPA was carried out using DBTTC as RAFT agent, and AIBN as initiator. Typically, solution copolymerization of *n*BuA (0.35 mL, 2.5 × 10^{-3} mol) with PFPA (0.39 mL, 2.5 × 10^{-3} mol) was carried out using AIBN (1.64 mg, 1.0 × 10^{-5} mol), DBTTC (29 mg, 1.0 × 10^{-4} mol) and DMF (0.7 mL) as solvent, also acting as an internal reference for the measurement of *n*BuA and PFPA consumption via ^{1}H NMR. A stock solution was typically transferred into a flask sealed with rubber septum, deoxygenated by nitrogen bubbling for ~30 min at 0 °C, then immersed in an oil bath thermostated at 65 °C. The reaction was stopped by plunging the flask into liquid nitrogen. The copolymer was subsequently precipitated twice into MeOH/H$_2$O (1/1, v/v) in order to eliminate residual *n*BuA and PFPA. The copolymer was dried under vacuum and characterized by ^{1}H NMR, ^{19}F NMR, SEC and ESI-TOF mass spectrometry. The molar mass of pure poly(*n*BuA-*co*-PFPA) was finally evaluated by ^{1}H NMR (CD$_2$Cl$_2$) from the relative integration of the characteristic ester group protons of the P*n*BuA backbone (-O-C*H$_2$*-CH$_2$-, 2mH, δ = 4.05 ppm, with m being the degree of polymerization), the PPFPA backbone (-O-C*H$_2$*-CF$_2$-, 2nH, δ = 4.58 ppm, with n being the degree of polymerization) and of the characteristic aromatic protons of DBTTC (ph*H*, 10H, δ = 7.15-7.38 ppm).

Copolymerization of *n*BuA with TFEA

Solution copolymerization of *n*BuA with TFEA was carried out using DBTTC as RAFT agent, and AIBN as initiator. Typically, solution copolymerization of *n*BuA (0.35 mL, 2.5 × 10^{-3} mol) with TFEA (0.31 mL, 2.5 × 10^{-3} mol) was carried out using AIBN (1.64 mg, 1.0 × 10^{-5} mol), DBTTC (29 mg, 1.0 × 10^{-4} mol) and DMF (0.6 mL) as solvent, also acting as an internal reference for the measurement of *n*BuA and TFEA consumption via ^{1}H NMR. A stock solution was typically transferred into a flask sealed with rubber septum, deoxygenated by nitrogen bubbling for ~30 min at 0 °C, then immersed in an oil bath thermostatted at 65 °C. The reaction was stopped by plunging the flask into liquid nitrogen. The copolymer was subsequently precipitated twice into MeOH/H$_2$O (1/1, v/v) in order to eliminate residual *n*BuA and TFEA. The copolymer was dried under vacuum and characterized by ^{1}H NMR, ^{19}F NMR, SEC and ESI-TOF mass

spectrometry. The molar mass of pure poly(*n*BuA-*co*-TFEA) was finally evaluated by ^{1}H NMR (CD$_2$Cl$_2$) from relative integration of the characteristic ester group protons of the P*n*BuA backbone (-O-C*H$_2$*-CH$_2$-, 2mH, δ = 4.05 ppm, with m being the degree of polymerization), the PTFEA backbone (-O-C*H$_2$*-CF$_3$, 2nH, δ = 4.51 ppm, with n being the degree of polymerization) and of the characteristic aromatic protons of DBTTC (ph*H*, 10H, δ = 7.15-7.38 ppm).

Results and discussions

Aiming at generating a new series of well-defined semifluorinated copolymers, RAFT copolymerization of *n*BuA with several semifluorinated acrylates, HFBA, PFPA or TFEA, were carried out (see **Scheme 1**). The copolymerization kinetics of *n*BuA with HFBA, PFPA or TFEA to predict the microstructure of each pair of co-monomers were studied by Fineman-Ross and Kelen-Tüdos laws. In order to minimize the amount of (co)polymer chains bearing a thermal initiator adduct while still maintaining a reasonable polymerization kinetic, the DBTTC to initiator (AIBN) ratio of all the (co)polymerizations was maintained as 10.

Homopolymerization of HFBA

Prior to investigating the incorporation of *n*BuA into the semifluorinated polymer chains, DBTTC, which is especially suited for the controlled polymerization of acrylate monomers,[54] the DBTTC-homopolymerization of HFBA was firstly conducted to gain a preliminary understanding about the RAFT polymerization kinetics (see **Scheme S1**).

The number-average molecular weights and the corresponding molecular weight distribution of the obtained homopolymer, PHFBA, are given in **Table 1**. As shown in **Table 1** and **Figure 1**, solution homopolymerization of HFBA in the

Table 1: Properties of the RAFT-made semifluorinated PHFBA homopolymers.

Sample	[HFBA]/ [DBTTC]	*Conv*[a] %	*Mn* $_{th}$[b] g/mol	*Mn* $_{NMR}$[c] g/mol	*Mn* $_{SEC}$[d] g/mol	*PDI*[d]
PHFBA1	100	16.6	4500	6900	3700	1.30
PHFBA2	100	32.7	8500	10500	7100	1.27
PHFBA3	100	49.8	12900	15100	11500	1.19
PHFBA4	100	75.6	19500	24500	17300	1.23

[a]: Conversion from ^{1}H NMR. [b]: Number-average molecular weights were evaluated from the following equation: *Mn* $_{th}$ = Conv x ([M]/[CTA]) x m$_M$ + m$_{CTA}$. [c]: Determined from relative integration of protons from ^{1}H NMR. [d]: From RI signals of SEC in THF (PS calibration).
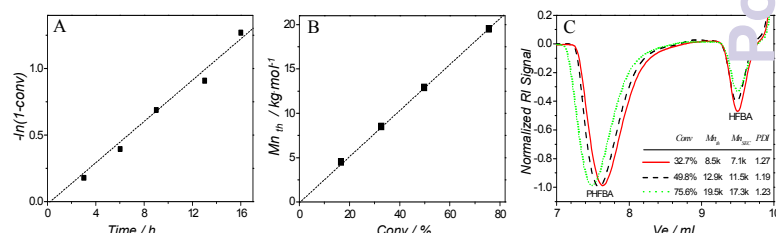
Figure 1: Semifluorinated PHFBA homopolymer. (A) First-order kinetic plots and (B) *Mn* $_{th}$ versus conversion (C) Evolution of the normalized RI signals of SEC

traces for the solution homopolymerization of HFBA in DMF at 65°C, mediated by DBTTC using AIBN as initiator: [M]/[CTA] = 100, [CTA]/[Initiator] = 10.
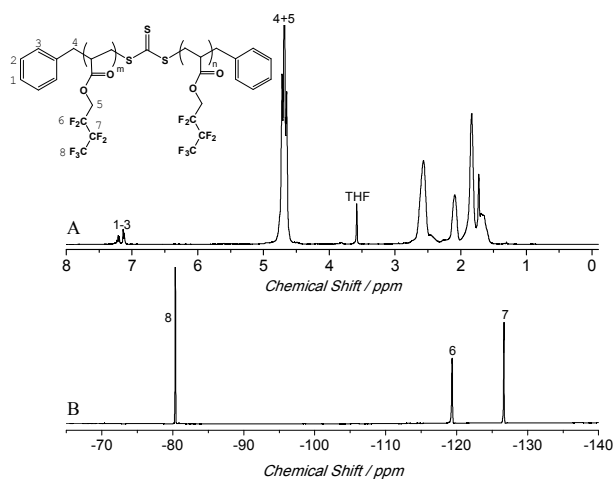
Figure 2: ^{1}H- (A) and ^{19}F- (B) NMR spectra of semifluorinated PHFBA homopolymer, recorded in THF-d$_8$ at 50 ^{o}C.

presence of DBTTC illustrated a controlled manner. Kinetic studies highlighted a linear relationship between -ln(1-x) and time (**Figure 1**A). Moreover, the theoretical molar mass (Mn_{th}) of polymer chains grew linearly with co-monomer conversion (**Figure 1**B). As expected, a negative refractive index (RI) response of the SEC traces (relative to THF) was obtained (**Figure 1**C) and the PDI remained below 1.3. The good correlation between the theoretical molecular weight and the experimental values obtained from SEC and ^{1}H NMR analysis (**Table 1**) also confirmed the controlled/living character of the polymerizations.

Polymer analysis was subsequently performed by ^{1}H and ^{19}F NMR spectroscopy in THF-d$_8$. Characteristic protons of the DBTTC and PHFBA (**Figure 2**A), as well as the fluorines of PHFBA (**Figure 2**B) were visualized and assigend for all the synthesized homopolymers.

Copolymerization of *n*BuA with HFBA, PFPA or TFEA

After demonstrating the usability of DBTTC, its ability to grow copolymer chains in a controlled manner was examined. Firstly, DBTTC-mediated solution copolymerization of *n*BuA with HFBA was carried out in DMF at 65 ^{o}C. Co-monomer conversion versus time plots are given in **Figure 3**A: thus copolymerization proceeded with pseudo-first-order kinetics, indicating a constant number of propagating centres. Moreover, Mn_{th} grew linearly with co-monomer conversion (**Figure 3**B). The resultant copolymers poly(*n*BuA-*co*-HFBA) were subsequently analysed by SEC, yielding partially negative and partially positive signals from RI detector (**Figure 3**C), probably resulting from the combination of fluorinated and non-fluorinated monomers along the copolymers backbone. As unfortunately it was impossible to deduce the accurate molecular weight relying on these RI signals, a UV detector directly connected to the SEC was employed. As can be seen in **Figure 3**D, the UV response of the semifluorinated copolymers

exhibited positive and monomodal peaks, which progressively shifted towards higher molecular weight with conversion, indicating a good agreement between theoretical molar masses (Mn_{th}) and the experimental ones (Mn_{SEC}, Mn_{NMR}), together with low PDI's, all indicative of the controlled manner of the copolymerizations (**Table 2**).

Encouraged by the successful copolymerization of *n*BuA with HFBA using DBTTC, the RAFT copolymerizations of *n*BuA with PFPA and TFEA were subsequently carried out under the same conditions. Consistent with a controlled copolymerization process, linear first order kinetic plots (**Figure 3**E&H) were obtained for both the resulting semifluorinated copolymers, poly(*n*BuA-*co*-PFPA) and poly(*n*BuA-*co*-TFEA), with Mn_{th} growing linearly with co-monomers conversion (**Figure 3**F&I). Moreover, monomodal SEC traces and narrow molecular weight distributions were obtained in both cases (**Figure 3**G&J). As expected, experimental molecular weights obtained from ^{1}H NMR and SEC analysis fitted very well with theoretical values (**Table 2**). Copolymer analysis was subsequently performed by ^{1}H- and ^{19}F-NMR spectroscopy in CD$_2$Cl$_2$ at 27 ^{o}C (**Figure 4**). In all cases,
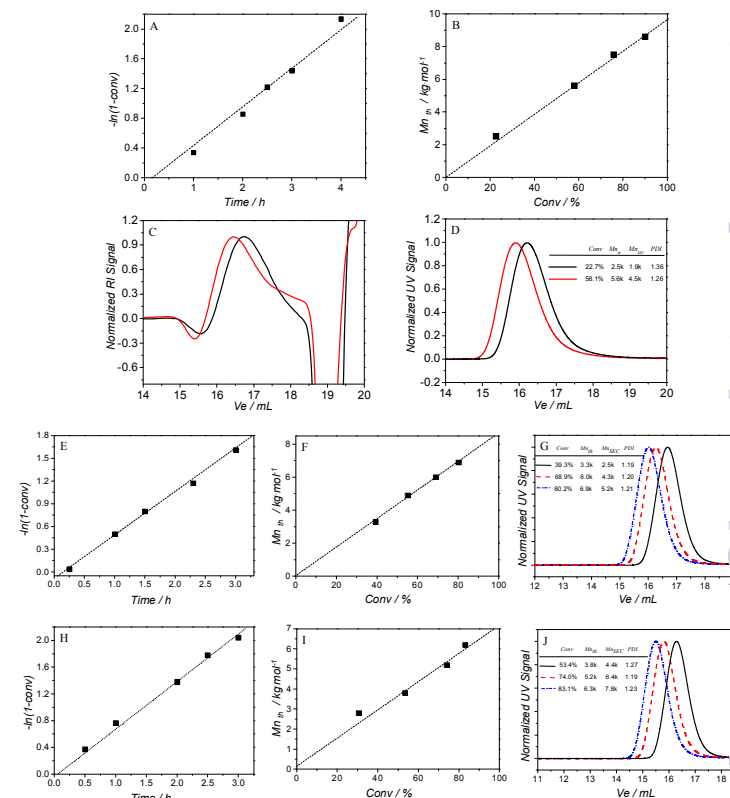
Figure 3: (A) Pseudo first-order kinetic plots, (B) Mn_{th} versus conversion (C) evolution of the normalized RI signals and (D) evolution of the normalized UV signals for the copolymerization of *n*BuA with HFBA in DMF at 65°C. (E) Pseudo first-order kinetic plots, (F) Mn_{th} versus conversion and (G) evolution of the normalized UV signals for the copolymerization of *n*BuA with PFPA in DMF at 65°C. (H) Pseudo first-order kinetic plots, (I) Mn_{th} versus conversion and (J) evolution of the normalized UV signals for the copolymerization of *n*BuA with TFEA in DMF at 65°C. In all cases, [M]/[CTA] = 50, [CTA]/[Initiator] = 10 The wavelength of absorption (305nm) for copolymers was determined by UV-spectroscopy.

Table 2: Experimental properties of the RAFT-made semifluorinated copolymers: poly(*n*BuA-*co*-HFBA), poly(*n*BuA-*co*-PFPA) and poly(*n*BuA-*co*-TFEA).

Sample	CTA	[M]/[CTA]	f	Conv[d] %	F	Mn_{th}[h] g/mol	Mn_{NMR}[i] g/mol	Mn_{SEC}[j] g/mol	PDI[j]
poly(*n*BuA-*co*-HFBA)1	DBTTC	50	0.560[a]	22.7	0.559[e]	2500	4100	1900	1.36
poly(*n*BuA-*co*-HFBA)2	DBTTC	50	0.560[a]	58.1	0.558[e]	5600	7300	4500	1.26
poly(*n*BuA-*co*-HFBA)3	DBTTC	50	0.560[a]	75.9	0.552[e]	7500	9600	6300	1.23
poly(*n*BuA-*co*-HFBA)4	DBTTC	50	0.560[a]	90.2	0.548[e]	8600	11300	7800	1.25
poly(*n*BuA-*co*-HFBA)5	DBTTC	450	0.485[a]	48.9	0.476[e]	43800	48700	39700	1.27
poly(*n*BuA-*co*-PFPA)1	DBTTC	50	0.50[b]	39.3	0.500[f]	3300	4600	2500	1.19
poly(*n*BuA-*co*-PFPA)2	DBTTC	50	0.50[b]	55.1	0.499[f]	4900	5700	3800	1.20
poly(*n*BuA-*co*-PFPA)3	DBTTC	50	0.50[b]	68.9	0.498[f]	6000	6800	4300	1.20
poly(*n*BuA-*co*-PFPA)4	DBTTC	50	0.50[b]	80.2	0.498[f]	6900	7300	5200	1.21
poly(*n*BuA-*co*-PFPA)5	DBTTC	450	0.442[b]	45.7	0.439[f]	34700	37900	29300	1.22
poly(*n*BuA-*co*-TFEA)1	DBTTC	50	0.466[c]	30.6	0.469[g]	2900	5300	4000	1.31
poly(*n*BuA-*co*-TFEA)2	DBTTC	50	0.466[c]	53.4	0.470[g]	3800	6100	4400	1.27
poly(*n*BuA-*co*-TFEA)3	DBTTC	50	0.466[c]	74.0	0.471[g]	5200	7500	6400	1.19
poly(*n*BuA-*co*-TFEA)4	DBTTC	50	0.466[c]	83.1	0.471[g]	6300	8900	7800	1.23
poly(*n*BuA-*co*-TFEA)5	DBTTC	450	0.492[c]	40.6	0.501[g]	26400	31200	21800	1.26

[a]: Initial molar fraction of HFBA in the co-monomer mixture. [b]: Initial molar fraction of PFPA in the co-monomer mixture. [c]: Initial molar fraction of TFEA in the co-monomer mixture. [d]: Overall commoner conversion from ^{1}H NMR. [e]: Molar fraction of HFBA in the final copolymers, poly(*n*BuA-*co*-HFBA), calculated from ^{1}H NMR. [f]: Molar fraction of HFBA in the final copolymer, poly(*n*BuA-*co*-HFBA), calculated from ^{1}H NMR. [g]: Molar fraction of HFBA in the final copolymer, poly(*n*BuA-*co*-HFBA), calculated from ^{1}H NMR. [h]: Number-average molecular weight was evaluated from the following equation: Mn_{th} = Conv x ([M]/[CTA]) x m_M + m_{CTA}. [i]: Determined from relative integration of protons from ^{1}H NMR. [j]: From UV signals of SEC in THF (PS calibration).
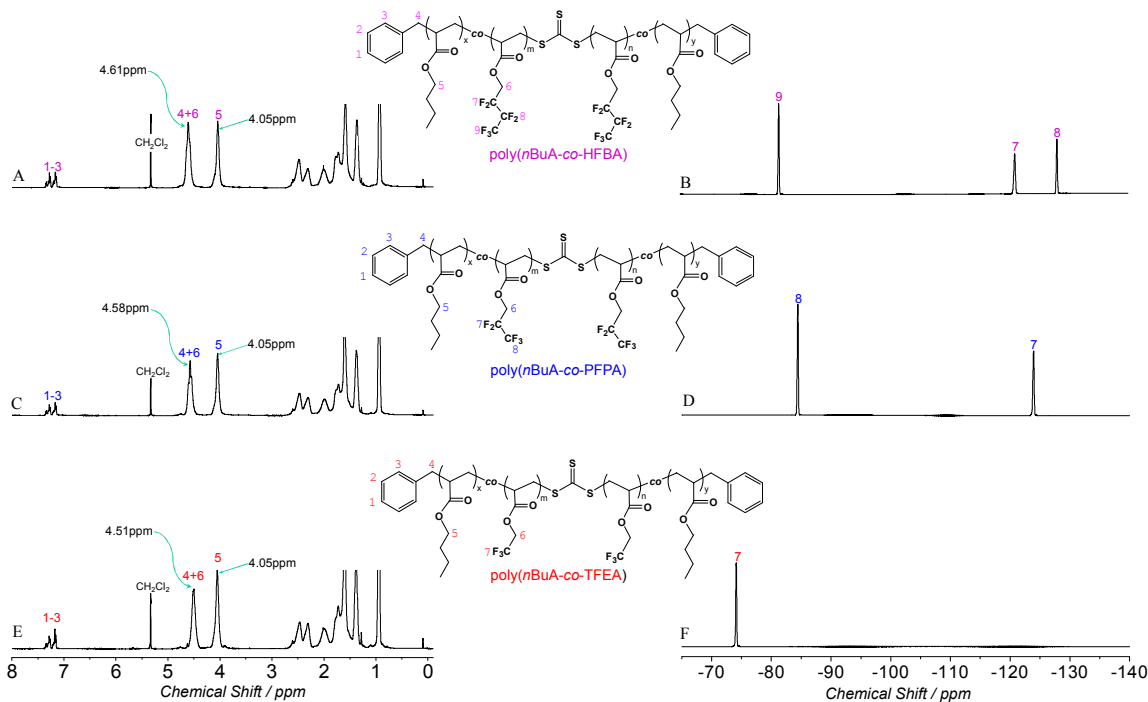
Figure 4: ^{1}H (A) and ^{19}F (B) NMR spectra of the semifluorinated poly(*n*BuA-*co*-HFBA) copolymer; ^{1}H (C) and ^{19}F (D) NMR spectra of the semifluorinated poly(*n*BuA-*co*-PFPA) copolymer; ^{1}H (E) and ^{19}F (F) NMR spectra of the semifluorinated poly(*n*BuA-*co*-TEEA) copolymer. Recorded in CD$_2$Cl$_2$ at 27 ^{o}C.

the characteristic protons of DBTTC and P*n*BuA, together with PHFBA (**Figure 4**A), PPFPA (**Figure 4**C) or PTFEA (**Figure 4**E), as well as the fluorines of PHFBA (**Figure 4**B), PPFPA (**Figure 4**D) or PTFEA (**Figure 4**F) were visualized for all the synthesized copolymers. It is also noteworthy that the -OC*H$_2$*-moieties of the PHFBA, PPFPA and PTFEA - copolymers displayed very similar chemical shift (4.61/4.58/4.51 ppm in **Figure 4**A,C,E, respectively).

One of the objectives of our work was to evaluate the composition of the semifluorinated copolymers relying on mass spectrometry - note the easiest task as current MALDI-TOF MS techniques have several limitations for the (semi)fluorinated (co)polymer analysis.[56] Interestingly, we found that ESI-TOF MS was particularly useful for readily analysing our semifluorinated copolymers, without using any added salts.

Firstly, the obtained semifluorinated copolymer, poly(*n*BuA-*co*-HFBA), was characterized by ESI-TOF MS spectroscopy (**Figure 5**) using MeOH as solvent. As shown in **Figure 5**A we observed in the negative-ion mode, illustrating the presence of singly charged negative main series (series ②, ⑧, ⑮ and ⑳), along with a range of other minor series (①, ③-⑦, ⑨-⑭ and ⑯-⑲) as seen in **Figure 5**B. The anions were separated due to their different ions and/or composition of *n*BuA and HFBA units. The mass difference between the m/z values of molecular ions in each main series (series ②, ⑧, ⑮ and ⑳) was equal to ~125.9 or ~128.1 g/mol, corresponding to the difference between molecular mass of individual *n*BuA (~128.1 g/mol) and HFBA (~254.1 g/mol) units. Main series numbered ②, ⑧, ⑮ and ⑳ can be attributed to the copolymers with the following numbers of *n*BuA/HFBA units: 5/2, 4/3, 5/3 and 6/3, respectively. The observed isotopic patterns (m/z) of the main series ② at m/z = 1561.3804 g/mol, is indicative of the assigned species $[(C_7H_7)_2(C_7H_{12}O_2)_5(C_7H_5F_7O_2)_2CS_3 - H_2 + Na_2 + Br]^-$ and the simulated pattern, m/z = 1561.3618 g/mol (**Figure 5**C). The observed isotopic patterns (m/z) of other main and minor series (①, ③-⑳, as seen in **Figure 5**B and **Table S1**) also matched well with the simulated structures. The presence of other ions in the spectrum (such as Na^+ and K^+) probably was a result of contamination from glassware or the use of synthetic grade solvents during the preparative path.

① : $[(C_7H_7)_2(C_7H_{12}O_2)_5(C_7H_5F_7O_2)_2CS_3 + H + Br + Cl]^-$

② : $[(C_7H_7)_2(C_7H_{12}O_2)_5(C_7H_5F_7O_2)_2CS_3 - H_2 + Na_2 + Br]^-$

③ : $[(C_7H_7)_2(C_7H_{12}O_2)_5(C_7H_5F_7O_2)_2CS_3 - H_2 + Na + K + Br]^-$

④ : $[(C_7H_7)_2(C_7H_{12}O_2)_5(C_7H_5F_7O_2)_2CS_3 + H + Br_2]^-$

⑤ : $[(C_7H_7)_2(C_7H_{12}O_2)_7(C_7H_5F_7O_2)_1CS_3 - H_4 + Na_3 + K + Br]^-$

⑥ : $[(C_7H_7)_2(C_7H_{12}O_2)_5(C_7H_5F_7O_2)_2CS_3 - H_4 + Na_2 + K_2 + Br]^-$

⑦ : $[(C_7H_7)_2(C_7H_{12}O_2)_4(C_7H_5F_7O_2)_3CS_3 + H + Br + Cl]^-$

⑧ : $[(C_7H_7)_2(C_7H_{12}O_2)_4(C_7H_5F_7O_2)_3CS_3 - H_2 + Na_2 + Br]^-$

⑨ : $[(C_7H_7)_2(C_7H_{12}O_2)_4(C_7H_5F_7O_2)_3CS_3 - H_2 + Na + K + Br]^-$

⑩ : $[(C_7H_7)_2(C_7H_{12}O_2)_4(C_7H_5F_7O_2)_3CS_3 + H + Br_2]^-$

⑪ : $[(C_7H_7)_2(C_7H_{12}O_2)_6(C_7H_5F_7O_2)_2CS_3 + (CH_3OH)_3 + Br]^-$

⑫ : $[(C_7H_7)_2(C_7H_{12}O_2)_6(C_7H_5F_7O_2)_2CS_3 - H_4 + Na_3 + K + Br]^-$

⑬ : $[(C_7H_7)_2(C_7H_{12}O_2)_4(C_7H_5F_7O_2)_3CS_3 - H_4 + Na_2 + K_2 + Br]^-$

⑭ : $[(C_7H_7)_2(C_7H_{12}O_2)_3(C_7H_5F_7O_2)_4CS_3 + H + Br + Cl]^-$

⑮ : $[(C_7H_7)_2(C_7H_{12}O_2)_5(C_7H_5F_7O_2)_3CS_3 - H_2 + Na_2 + Br]^-$

⑯ : $[(C_7H_7)_2(C_7H_{12}O_2)_5(C_7H_5F_7O_2)_3CS_3 + H + Br_2]^-$

⑰ : $[(C_7H_7)_2(C_7H_{12}O_2)_5(C_7H_5F_7O_2)_3CS_3 - H_4 + Na_3 + K + Br]^-$

⑱ : $[(C_7H_7)_2(C_7H_{12}O_2)_5(C_7H_5F_7O_2)_3CS_3 - H_4 + Na_2 + K_2 + Br]^-$

⑲ : $[(C_7H_7)_2(C_7H_{12}O_2)_4(C_7H_5F_7O_2)_4CS_3 + H + Br + Cl]^-$

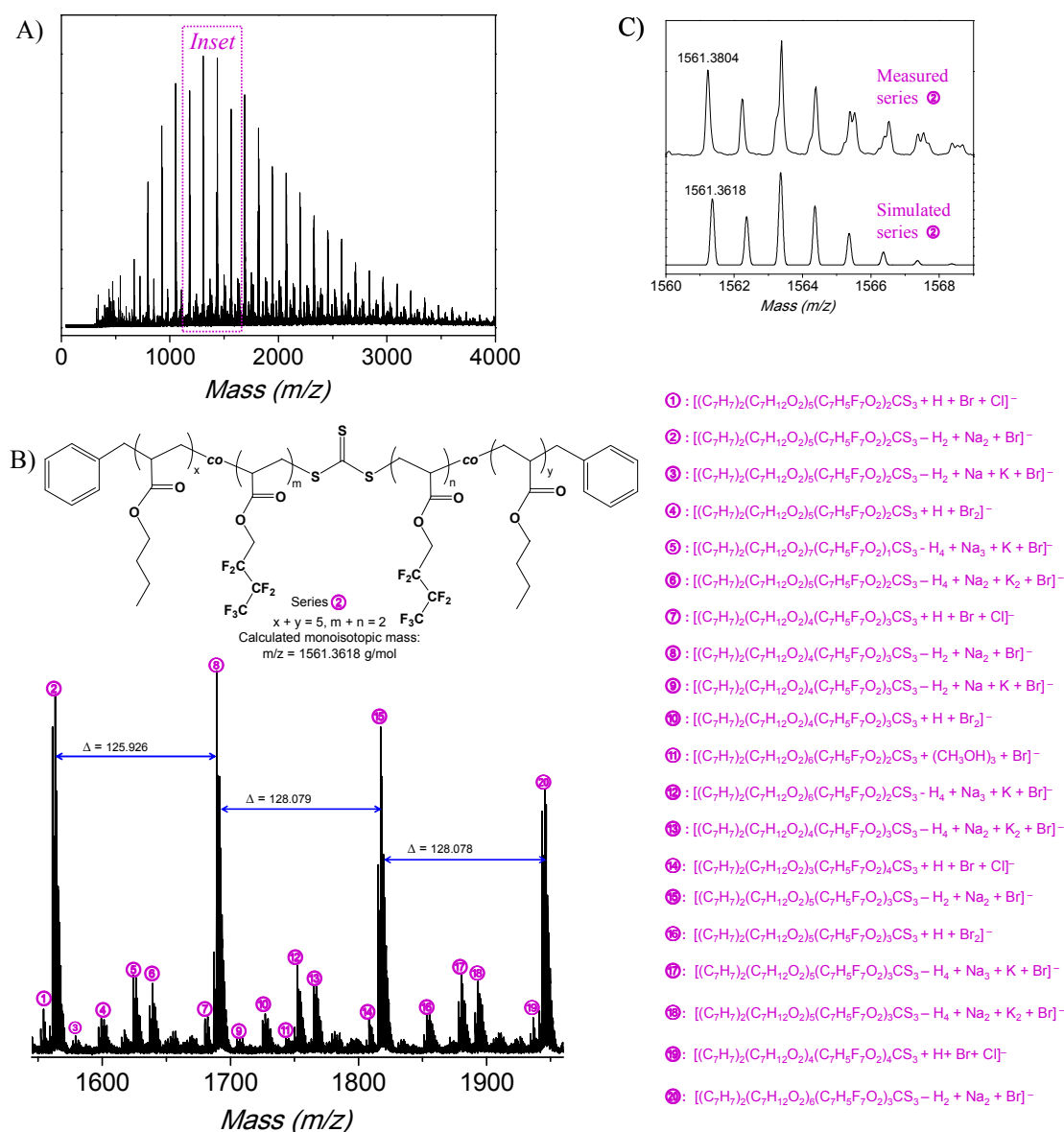⑳ : $[(C_7H_7)_2(C_7H_{12}O_2)_6(C_7H_5F_7O_2)_3CS_3 - H_2 + Na_2 + Br]^-$

Figure 5: ESI-TOF MS of the poly(*n*BuA-*co*-HFBA) copolymer. (A) full spectrum, (B) expansion and (C) simulation of the isotope pattern.

Based on the successful ESI-TOF MS measurement of poly(*n*BuA-*co*-HFBA), we subsequently analysed another semifluorinated poly(*n*BuA-*co*-PFPA) copolymer (**Figure 6**), using MeOH as solvent. **Figure 6**A was observed in the positive- ion mode, generating only singly charged species (1+). The ESI-TOF spectrum illustrated the presence of positive main series (series ①, ⑩, ⑭ and ⑳), along with other minor series (②-⑨, ⑪-⑬ and ⑮-⑲) as seen in **Figure 6**B. The ions were separated due to their different ions and/or composition of *n*BuA and PFPA units. The mass difference between the m/z values of molecular ions in each main series (series ①, ⑩, ⑭ and ⑳) was equal to ~75.9 g/mol, which was corresponding to the difference between molecular mass of individual *n*BuA

(~128.1 g/mol) and PFPA (~204.0 g/mol) units, or ~52.0 g/mol, resulting from the different composition of *n*BuA and PFPA along the copolymer backbone. Main series ①, ⑩, ⑭ and ⑳ corresponded to the copolymers with the following numbers of *n*BuA/PFPA units: 6/3, 5/4, 7/3 and 6/4, respectively. The observed isotopic patterns (m/z) of main series ① located at m/z = 1693.5583 g/mol, corresponding to the assigned species $[(C_7H_7)_2(C_7H_{12}O_2)_6(C_6H_5F_5O_2)_3CS_3 + Na]^+$ and the simulated pattern, m/z = 1693.5803 (**Figure 6**C). The observed isotopic patterns (m/z) of other main and minor series (②-⑳, as seen in **Figure 6**B and **Table S2**), also matched well with the simulated structures.

① : $[(C_7H_7)_2(C_7H_{12}O_2)_6(C_6H_5F_5O_2)_3CS_3 + Na]^+$

② : $[(C_7H_7)_2(C_7H_{12}O_2)_6(C_6H_5F_5O_2)_3CS_3 - H + Li + Na]^+$

③ : $[(C_7H_7)_2(C_7H_{12}O_2)_6(C_6H_5F_5O_2)_3CS_3 + K]^+$

④ : $[(C_7H_7)_2(C_7H_{12}O_2)_3(C_6H_5F_5O_2)_5CS_3 + Na]^+$

⑤ : $[(C_7H_7)_2(C_7H_{12}O_2)_3(C_6H_5F_5O_2)_5CS_3 - H + Li + Na]^+$

⑥ : $[(C_7H_7)_2(C_7H_{12}O_2)_3(C_6H_5F_5O_2)_5CS_3 + K]^+$

⑦ : $[(C_7H_7)_2(C_7H_{12}O_2)_8(C_6H_5F_5O_2)_2CS_3 + Na]^+$

⑧ : $[(C_7H_7)_2(C_7H_{12}O_2)_8(C_6H_5F_5O_2)_2CS_3 - H + Li + Na]^+$

⑨ : $[(C_7H_7)_2(C_7H_{12}O_2)_8(C_6H_5F_5O_2)_2CS_3 + K]^+$

⑩ : $[(C_7H_7)_2(C_7H_{12}O_2)_5(C_6H_5F_5O_2)_4CS_3 + Na]^+$

⑪ : $[(C_7H_7)_2(C_7H_{12}O_2)_5(C_6H_5F_5O_2)_4CS_3 - H + Li + Na]^+$

⑫ : $[(C_7H_7)_2(C_7H_{12}O_2)_5(C_6H_5F_5O_2)_4CS_3 + K]^+$

⑬ : $[(C_7H_7)_2(C_7H_{12}O_2)_5(C_6H_5F_5O_2)_4CS_3 - H + Li + K]^+$

⑭ : $[(C_7H_7)_2(C_7H_{12}O_2)_7(C_6H_5F_5O_2)_3CS_3 + Na]^+$

⑮ : $[(C_7H_7)_2(C_7H_{12}O_2)_7(C_6H_5F_5O_2)_3CS_3 + K]^+$

⑯ : $[(C_7H_7)_2(C_7H_{12}O_2)_4(C_6H_5F_5O_2)_5CS_3 + Na]^+$

⑰ : $[(C_7H_7)_2(C_7H_{12}O_2)_4(C_6H_5F_5O_2)_5CS_3 - H + Li + Na]^+$

⑱ : $[(C_7H_7)_2(C_7H_{12}O_2)_4(C_6H_5F_5O_2)_5CS_3 + K]^+$

⑲ : $[(C_7H_7)_2(C_7H_{12}O_2)_6(C_6H_5F_5O_2)_4CS_3 - H_2 + Li + Na + K]^+$

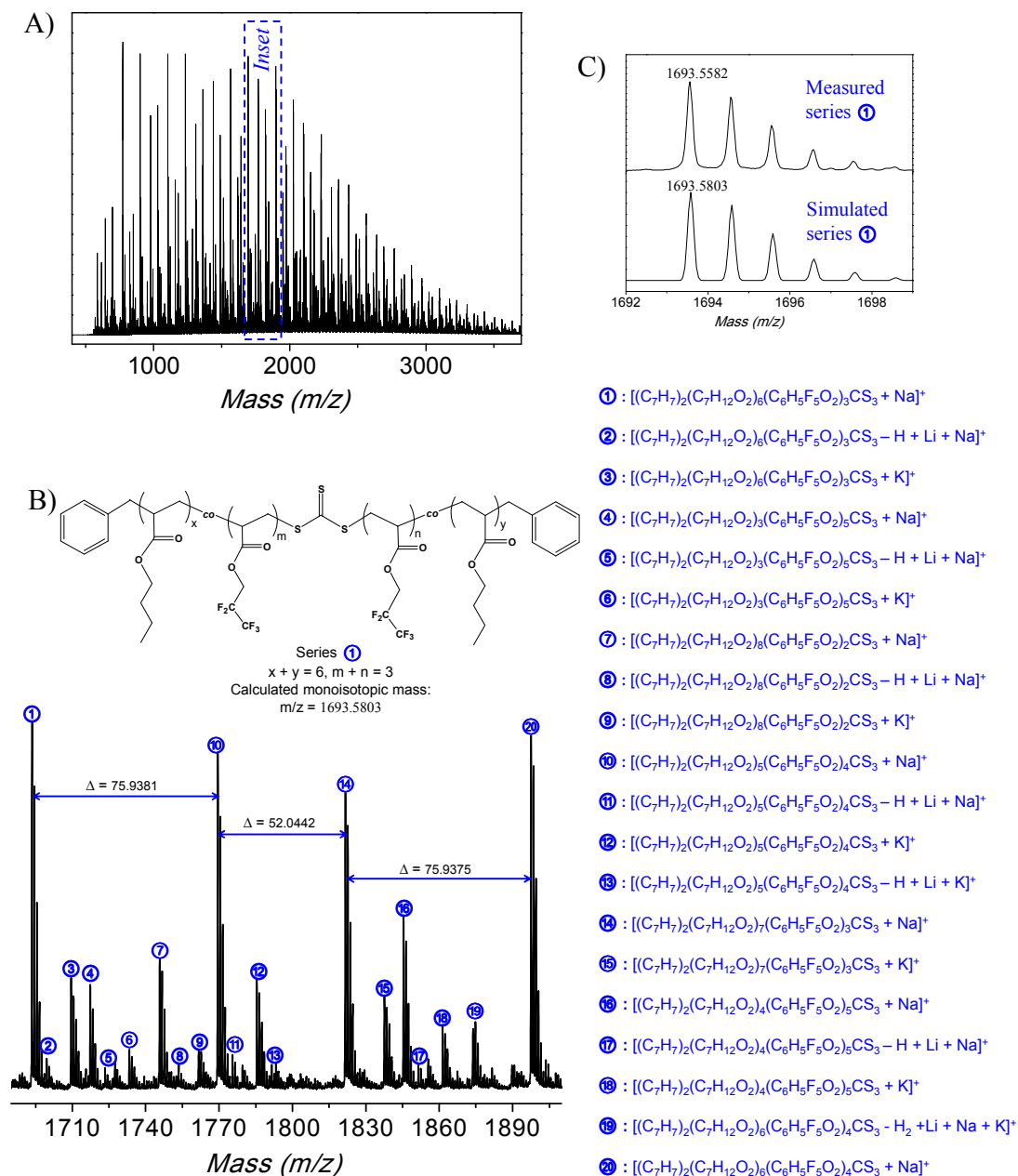⑳ : $[(C_7H_7)_2(C_7H_{12}O_2)_6(C_6H_5F_5O_2)_4CS_3 + Na]^+$

Figure 6: ESI-TOF MS of the poly(*n*BuA-*co*-PFPA) copolymer. (A) full spectrum, (B) expansion and (C) simulation of the isotope pattern.

In a similar manner, the obtained semifluorinated copolymer, poly(nBuA-co-TFEA), was further characterized by ESI-TOF MS spectroscopy (**Figure 7**) using MeOH as solvent. The ESI-TOF spectrum (see Figure 7A) illustrated the presence of singly charged positive main series (series ②, ⑤, ⑧, ⑪, ⑭, ⑰ and ⑳), along with other doubly charged minor series (①, ④, ⑦, ⑩, ⑬, ⑯ and ⑲) and overlapping of singly and doubly charged series (③, ⑥, ⑨, ⑫, ⑮ and ⑱) as seen in **Figure 7**B. The ions were separated due to their different ions and/or composition of nBuA and TFEA units. The mass difference between the m/z values of molecular ions in each main series (series ②, ⑤, ⑧, ⑪, ⑭, ⑰ and ⑳) was equal to ~25.9 or ~24.3 g/mol, which was corresponding to the difference between the molecular mass of individual nBuA (~128.1 g/mol) and TFEA (~154.0 g/mol) units. Main series ②, ⑤, ⑧, ⑪, ⑭, ⑰ and ⑳ corresponded to the copolymers with the following numbers of nBuA/TFEA units: 7/3, 6/4, 5/5, 4/6, 9/2, 8/3 and 7/4, respectively. The observed isotopic patterns (m/z) of main series ② located at m/z = 1761.6514 g/mol, corresponded to the assigned species $[(C_7H_7)_2(C_7H_{12}O_2)_7(C_5H_5F_3O_2)_3CS_3 + Na]^+$ and the simulated pattern, m/z = 1761.6736 g/mol (**Figure 7**C). The observed isotopic patterns (m/z) of other main and minor series (①, ③-⑳, as seen in **Figure 7**B and **Table S3**), also matched well with the simulated structures.

① : $[(C_7H_7)_2(C_7H_{12}O_2)_{15}(C_5H_5F_3O_2)_7CS_3 + 2Na]^{2+}$

② : $[(C_7H_7)_2(C_7H_{12}O_2)_7(C_5H_5F_3O_2)_3CS_3 + Na]^+$

③ : $[(C_7H_7)_2(C_7H_{12}O_2)_7(C_5H_5F_3O_2)_3CS_3 - H + Na + Li]^+$
 & $[(C_7H_7)_2(C_7H_{12}O_2)_{14}(C_5H_5F_3O_2)_8CS_3 + 2Na]^{2+}$

④ : $[(C_7H_7)_2(C_7H_{12}O_2)_{13}(C_5H_5F_3O_2)_9CS_3 + 2Na]^{2+}$

⑤ : $[(C_7H_7)_2(C_7H_{12}O_2)_6(C_5H_5F_3O_2)_4CS_3 + Na]^+$

⑥ : $[(C_7H_7)_2(C_7H_{12}O_2)_6(C_5H_5F_3O_2)_4CS_3 - H + Na + Li]^+$
 & $[(C_7H_7)_2(C_7H_{12}O_2)_{12}(C_5H_5F_3O_2)_{10}CS_3 + 2Na]^{2+}$

⑦ : $[(C_7H_7)_2(C_7H_{12}O_2)_{11}(C_5H_5F_3O_2)_{11}CS_3 + 2Na]^{2+}$

⑧ : $[(C_7H_7)_2(C_7H_{12}O_2)_5(C_5H_5F_3O_2)_5CS_3 + Na]^+$

⑨ : $[(C_7H_7)_2(C_7H_{12}O_2)_5(C_5H_5F_3O_2)_5CS_3 - H + Na + Li]^+$
 & $[(C_7H_7)_2(C_7H_{12}O_2)_{10}(C_5H_5F_3O_2)_{12}CS_3 + 2Na]^{2+}$

⑩ : $[(C_7H_7)_2(C_7H_{12}O_2)_9(C_5H_5F_3O_2)_{13}CS_3 + 2Na]^{2+}$

⑪ : $[(C_7H_7)_2(C_7H_{12}O_2)_4(C_5H_5F_3O_2)_6CS_3 + Na]^+$

⑫ : $[(C_7H_7)_2(C_7H_{12}O_2)_4(C_5H_5F_3O_2)_6CS_3 - H + Na + Li]^+$
 &$[(C_7H_7)_2(C_7H_{12}O_2)_8(C_5H_5F_3O_2)_{14}CS_3 + 2Na]^{2+}$

⑬ : $[(C_7H_7)_2(C_7H_{12}O_2)_7(C_5H_5F_3O_2)_{15}CS_3 + 2Na]^{2+}$

⑭ : $[(C_7H_7)_2(C_7H_{12}O_2)_9(C_5H_5F_3O_2)_2CS_3 + Na]^+$

⑮ : $[(C_7H_7)_2(C_7H_{12}O_2)_9(C_5H_5F_3O_2)_2CS_3 - H + Na + Li]^+$
 & $[(C_7H_7)_2(C_7H_{12}O_2)_6(C_5H_5F_3O_2)_{16}CS_3 + 2Na]^{2+}$

⑯ : $[(C_7H_7)_2(C_7H_{12}O_2)_5(C_5H_5F_3O_2)_{17}CS_3 + 2Na]^{2+}$

⑰ : $[(C_7H_7)_2(C_7H_{12}O_2)_8(C_5H_5F_3O_2)_3CS_3 + Na]^+$

⑱ : $[(C_7H_7)_2(C_7H_{12}O_2)_8(C_5H_5F_3O_2)_3CS_3 - H + Na + Li]^+$
 & $[(C_7H_7)_2(C_7H_{12}O_2)_4(C_5H_5F_3O_2)_{18}CS_3 + 2Na]^{2+}$

⑲ : $[(C_7H_7)_2(C_7H_{12}O_2)_3(C_5H_5F_3O_2)_{19}CS_3 + 2Na]^{2+}$

⑳ : $[(C_7H_7)_2(C_7H_{12}O_2)_7(C_5H_5F_3O_2)_4CS_3 + Na]^+$
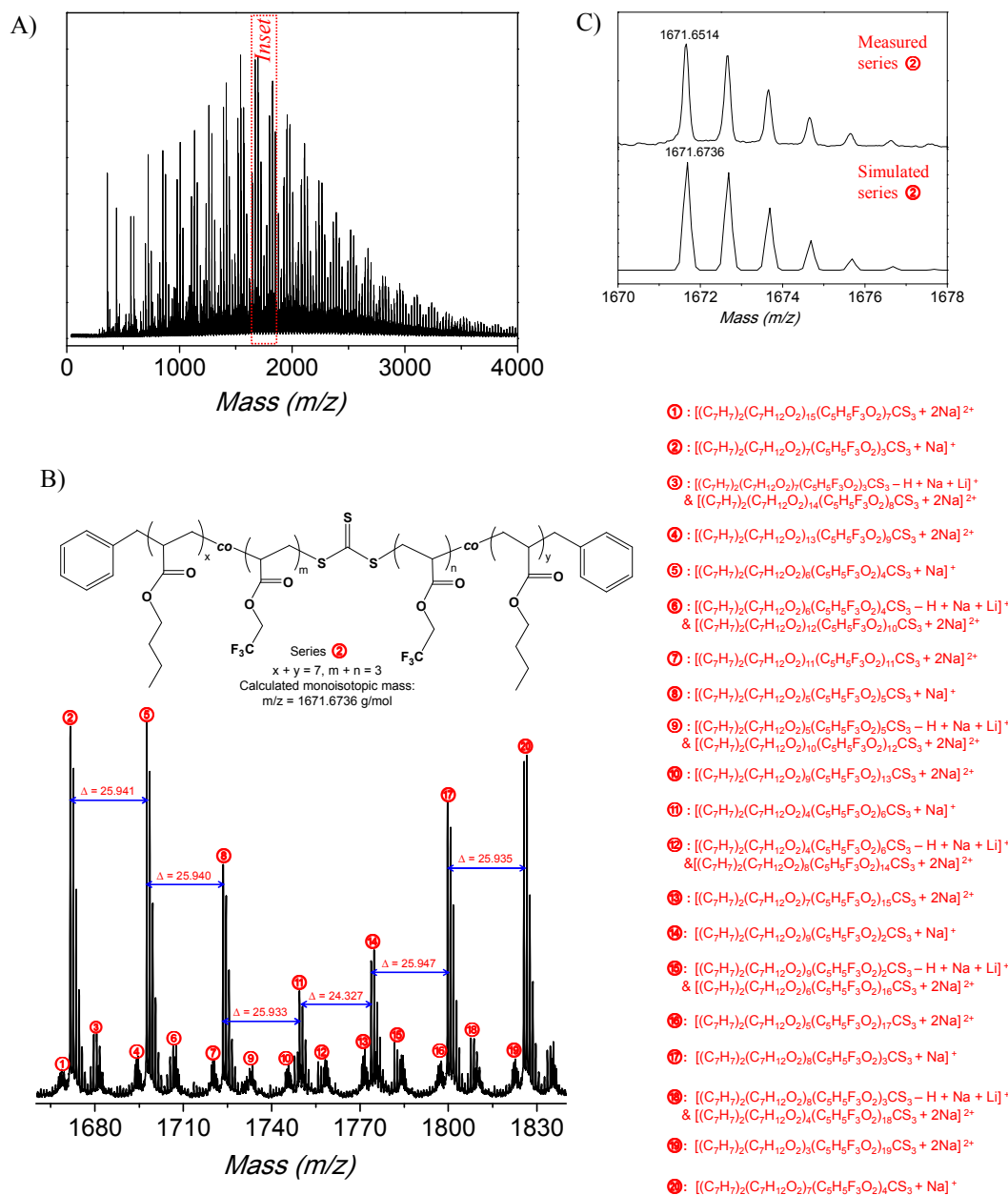
Figure 7: ESI-TOF MS of poly(nBuA-co-TFEA). (A) full spectrum, (B) expansion and (C) simulation of the isotope pattern.

It was another objective of our work to study the reactivity ratios of each pair of co-monomers: in this context, the reactivity ratios were assessed by well-established Fineman-Ross (RT)[57] and Kelen-Tüdos (KT)[58] laws from the composition of co-monomers in the feed (f) and in the copolymer (F) at low co-monomers conversion. Several experiments, from an initial co-monomer molar ratio ranging between about 20/80 and 80/20, were carried out at 65 °C in DMF (see **Table S4**, **5** and **6**). The copolymerizations were stopped after about 15 min to maintain a low co-monomer conversion (5-15%) calculated via ^{1}H NMR.

Table S4 summarized the different parameters to determine the reactivity ratios for the RAFT copolymerization of nBuA with HFBA from Fineman-Ross and Kelen-Tüdos laws. As expected, the plot of G versus H gives a linear relationship (**Figure S2**, left), where the slope (1.11) is corresponding to $r_{n\mathrm{BuA}}$ while the intercept (-0.93) yields -r_{HFBA} (**Table 3**). Another commonly method employed to evaluate the copolymerization reactivity ratios was derived by Kelen and Tüdos, by plotting η versus ζ leading to another linear relationship (**Figure S2**, right), where $r_{n\mathrm{BuA}}$ and $(-r_{\mathrm{HFBA}}/\alpha)$ are the values of η for ζ=1 and ζ = 0, respectively, i.e. $r_{n\mathrm{BuA}}$ = 1.08 and r_{HFBA} = 0.95.

The average of the values deduced from both the FR and KT laws yielded $\overline{r}_{n\mathrm{BuA}}$ = 1.10 and $\overline{r}_{\mathrm{HFBA}}$ = 0.94 at 65 °C, as seen in **Table 3**. Compared to the reactivity ratio of HFBA (r_{HFBA} = 0.94), the higher value of nBuA ($r_{n\mathrm{BuA}}$ = 1.10) indicates that the obtained semifluorinated copolymers contain more nBuA than HFBA in the backbone. In addition, the product ($r_{n\mathrm{BuA}} \times \overline{r}_{\mathrm{HFBA}}$) yielded 1.03 for poly($n$BuA-$co$-HFBA) copolymers, which was closed to unity, illustrating an almost similar relative reactivities of the two monomers, suggesting a random distribution of both co-monomers along the semifluorinated copolymer chains[59] in accordance with a very recent report.[60]

Similar, the reactivity ratios of nBuA and PFPA were also determined by FR and KT laws (**Table S5**). The monomer reactivity ratios were found to be $r_{n\mathrm{BuA}}$ = 0.96, r_{PFPA} = 1.13 with FR laws (**Table 3** and **Figure S3**, left), and $r_{n\mathrm{BuA}}$ = 0.92, r_{PFPA} = 1.07 with KT laws (**Table 3** and **Figure S3**, right). The average of the values yielded $\overline{r}_{n\mathrm{BuA}}$ = 0.94 and $\overline{r}_{\mathrm{PFPA}}$ = 1.10 at 65 °C, as seen in **Table 3**, indicating very close reactivity ratios of nBuA and PFPA: thus nearly ideal behaviour of the copolymerization ($\overline{r}_{n\mathrm{BuA}} \times \overline{r}_{\mathrm{TFEA}}$ = 1.12) for the poly(nBuA-co-PFPA) copolymers, and a random distribution of co-monomers along the obtained copolymers backbone can be

deducted.

In the case of the nBuA/TFEA couple (see **Table S6**), we found $r_{n\mathrm{BuA}}$ = 0.79, r_{TFEA} = 1.45 with FR laws (**Table 3** and **Figure S4**, left), and $r_{n\mathrm{BuA}}$ = 0.76, r_{TFEA} = 1.36 with KT laws (**Table 3** and **Figure S4**, right). The average of the values yielded $\overline{r}_{n\mathrm{BuA}}$ = 0.78 and $\overline{r}_{\mathrm{TFEA}}$ = 1.41 at 65 °C, indicating that TFEA ($\overline{r}_{\mathrm{TFEA}}$ = 1.41) was slightly more reactive than nBuA. The product ($r_{n\mathrm{BuA}} \times \overline{r}_{\mathrm{TFEA}}$) = 1.10 for the poly($n$BuA-$co$-TFEA) copolymers, demonstrated an nearly ideal copolymerizations,[59] thus expecting randomly arranged co-monomer units along the semifluorinated copolymer chains. which is also consistent with the hypothesis of other report.[61] It is also noteworthy that **Table 3** allowed us to arrange the relative reactivity of the monomers used in this work in the following order: TFEA > nBuA ≥ PFPA > HFBA.

Further evidence of a random structure of our obtained semifluorinated copolymers was given by the Q-e scheme (Q and e being attributed to the resonance and the polarity of monomer, respectively), which allows to predict the co-monomer distribution.[62] As seen in **Table 4**, the low $|e_{n\mathrm{BuA}} - e_{\mathrm{HFBA}}|$ difference (0.49 in this case) demonstrated a random structure of poly(nBuA-co-HFBA) copolymers. A similar conclusion was drawn in the case of nBuA/TFEA couple, as supported by the slight difference between e parameters ($|e_{n\mathrm{BuA}} - e_{\mathrm{TFEA}}|$ = 0.08).

Table 4: Selected Q and e values of monomers

Monomer	Q	e	Ref
nBuA	0.39	0.85	62
HFBA	0.96	1.34	62
TFEA	0.62	0.93	41

Conclusions

Taking advantage of controlled copolymerization mediated by DBTTC, a new series of semifluorinated copolymers, poly(nBuA-co-TFEA), poly(nBuA-co-PFPA) and poly(nBuA-co-HFBA), with controlled number-average molecular weight and low PDI's were successfully synthesized. Their chemical structure was characterized by a combination of ^{1}H, ^{19}F NMR, SEC and ESI-TOF MS spectrometry. Although current MALDI-TOF MS techniques have several limitations for the (semi)fluorinated (co)polymer analysis, we found that ESI-TOF MS was particularly useful for readily analysing our semifluorinated copolymers, without using any salt. The reactivity ratios of each co-monomer in the three pairs were further assessed by both Fineman-Ross and Kelen-Tüdos laws: in all cases the ($r_{\mathrm{M1}} \times r_{\mathrm{M2}}$) product was close to unity, indicating that all the copolymerizations were considered as close-to ideal, demonstrating a random distribution of each pair of co-monomers along the obtained copolymers backbone. The random structure of our semifluorinated copolymers were also confirmed relying on Q-e scheme. We envision that these fluorine-containing copolymers can lead to the development of new polymeric materials with improved solubility and modified

Table 3: Reactivity ratios of nBuA (r_{M1}) and co-monomers M_2 (r_{M2}) in RAFT copolymerization at 65 °C

M_2	r_{M1}		$\overline{r}_{M1}$ ^{a}	r_{M2}		$\overline{r}_{M2}$ ^{b}	$\overline{r}_{M1} \times \overline{r}_{M2}$
	FR	KT		FR	KT		
HFBA	1.11	1.08	1.10	0.93	0.95	0.94	1.03
PFPA	0.96	0.92	0.94	1.13	1.07	1.10	1.12
TFEA	0.79	0.76	0.78	1.45	1.36	1.41	1.10

^{a}: the average values of r_{M1} deduced from the FR and KT laws, ^{b}: the average values of r_{M2} deduced from the FR and KT laws.

surface properties. In order to study these possibilities further, additional studies are currently in progress which involve the incorporation of supramolecular chemistry and semifluorinated copolymers.

Acknowledgements

Notes and references

[a]: Institute of Chemistry, Chair of Macromolecular Chemistry, Faculty of Natural Sciences II (Chemistry, Physics and Mathematics), Martin-Luther University Halle-Wittenberg, von Danckelmann-Platz 4, Halle 06120, Germany. Email: wolfgang.binder@chemie.uni-halle.de.

Electronic Supplementary Information (ESI) available: [Synthetic route to semifluorinated homopolymer PHFBA, partial SEC traces of normalized UV signals for the obtained semifluorinated copolymers, ESI-TOF MS results of poly(*n*BuA-*co*-HFBA), poly(*n*BuA-*co*-PFPA) and poly(*n*BuA-*co*-TFEA), the different parameters to determine the reactivity ratios for the RAFT copolymerization of *n*BuA with HFBA, PFPA or TFEA, as well as Fineman-Ross graphic method [G = f(H)], and Kelen-Tüdos graphic method for each pair of co-monomers]. See DOI: 10.1039/b000000x/

1. Hirao, A.; Sugiyama, K.; Yokoyama, H. *Prog. Polym. Sci.* **2007,** 32, (12), 1393-1438.

2. Hansen, N. M. L.; Jankova, K.; Hvilsted, S. *Eur. Polym. J.* **2007,** 43, (2), 255-293.

3. Hvilsted, S. *Polym. Int.* **2014,** 63, (5), 814-823.

4. Boutevin, B.; Ameduri, B. *Macromol. Symp.* **1994,** 82, (1), 1-17.

5. Ameduri, B.; Boutevin, B. *Well-Architectured Fluoropolymers: Synthesis, Properties and Applications* **2004**, Elsevier: Amsterdam.

6. Moore, A. L. *Fluoroelastomers Handbook; the Definitive User's Guide and Data Book* **2006**, Plastic Design Library; William Andrew Publishing: Norwich, NY.

7. Babudri, F.; Farinola, G. M.; Naso, F.; Ragni, R. *Chem. Commun.* **2007**, (10), 1003-1022.

8. Patil, Y.; Ameduri, B. *Prog. Polym. Sci.* **2013,** 38, (5), 703-739.

9. Ameduri, B. *Macromolecules.* **2010,** 43, (24), 10163-10184.

10. Boschet, F.; Ameduri, B. *Chem. Rev.* **2013,** 114 (2), 927-980.

11. Percec, V.; Wang, J. H.; Oishi, Y.; Feiring, A. E. *J. Polym. Sci., Part A: Polym. Chem.* **1991,** 29, (7), 965-976.

12. Hirao, A.; Koide, G.; Sugiyama, K. *Macromolecules.* **2002,** 35, (20), 7642-7651.

13. Hirao, A.; Sakai, S.; Sugiyama, K. *Polym. Advan. Technol.* **2004,** 15, (1-2), 15-25.

14. Yokoyama, H.; Tanaka, K.; Takahara, A.; Kajiyama, T.; Sugiyama, K.; Hirao, A. *Macromolecules.* **2003,** 37, (3), 939-945.

15. El-Shehawy, A. A.; Yokoyama, H.; Sugiyama, K.; Hirao, A. *Macromolecules.* **2005,** 38, (20), 8285-8299.

16. Ishizone, T.; Sugiyama, K.; Sakano, Y.; Mori, H.; Hirao, A.; Nakahama, S. *Polym. J.* **1999,** 31, (11_2), 983-988.

17. Abouelmagd, A.; Sugiyama, K.; Hirao, A. *Macromolecules.* **2011,** 44, (4), 826-834.

18. Höpken, J.; Möller, M.; Lee, M.; Percec, V. *Die Makromolekulare Chemie* **1992,** 193, (1), 275-284.

19. Percec, V.; Tomazos, D.; Feiring, A. E. *Polymer* **1991,** 32, (10), 1897-1908.

20. Liu, W.; Nakano, T.; Okamoto, Y. *J. Polym. Sci., Part A: Polym. Chem.* **2000,** 38, (6), 1024-1032.

21. Hirano, T.; Furutani, T.; Oshimura, M.; Ute, K. *J. Polym. Sci., Part A: Polym. Chem.* **2012,** 50, (12), 2471-2483.

22. Patil, Y.; Hori, H.; Tanaka, H.; Sakamoto, T.; Ameduri, B. *Chem. Commun.* **2013,** 49, (59), 6662-6664.

23. Xia, J.; Johnson, T.; Gaynor, S. G.; Matyjaszewski, K.; DeSimone, J. *Macromolecules.* **1999,** 32, (15), 4802-4805.

24. Perrier, S.; Jackson, S. G.; Haddleton, D. M.; Améduri, B.; Boutevin, B. *Macromolecules.* **2003,** 36, (24), 9042-9049.

25. Hansen, N. M. L.; Haddleton, D. M.; Hvilsted, S. *J. Polym. Sci., Part A: Polym. Chem.* **2007,** 45, (24), 5770-5780.

26. Hansen, N. M. L.; Gerstenberg, M.; Haddleton, D. M.; Hvilsted, S. *J. Polym. Sci., Part A: Polym. Chem.* **2008,** 46, (24), 8097-8111.

27. Dimitrov, I.; Takamuku, S.; Jankova, K.; Jannasch, P.; Hvilsted, S. *Macromol. Rapid. Comm.* **2012,** 33, (16), 1368-1374.

28. Nielsen, M. M.; Ching-Ching Yang, A.; Jankova, K.; Hvilsted, S.; Holdcroft, S. *Journal of Materials Chemistry A* **2013,** 1, (28), 8118-8126.

29. O'Shea, J.-P.; Solovyeva, V.; Guo, X.; Zhao, J.; Hadjichristidis, N.; Rodionov, V. O. *Polym. Chem.* **2014,** 5, (3), 698-701.

30. Samanta, S.; Cai, R.; Percec, V. *Polym. Chem.* **2014**, DOI: 10.1039/C4PY00635F

31. Lacroix-Desmazes, P.; Andre, P.; Desimone, J. M.; Ruzette, A.-V.; Boutevin, B. *J. Polym. Sci., Part A: Polym. Chem.* **2004,** 42, (14), 3537-3552.

32. Eberhardt, M.; Théato, P. *Macromol. Rapid. Comm.* **2005,** 26, (18), 1488-1493.

33. Koiry, B. P.; Moukwa, M.; Singha, N. K. *J. Fluorine. Chem.* **2013,** 153, (0), 137-142.

34. Yang, K.; Huang, X.; Huang, Y.; Xie, L.; Jiang, P. *Chem. Mater.* **2013,** 25, (11), 2327-2338.

35. Nuhn, L.; Overhoff, I.; Sperner, M.; Kaltenberg, K.; Zentel, R. *Polym. Chem.* **2014,** 5, (7), 2484-2495.

36. Girard, E.; Marty, J.-D.; Ameduri, B.; Destarac, M. *ACS Macro Lett.* **2012,** 1, (2), 270-274.

37. Shimizu, T.; Tanaka, Y.; Kutsumizu, S.; Yano, S. *Macromolecules.* **1993,** 26, (24), 6694-6696.

38. Shimizu, T.; Tanaka, Y.; Kutsumizu, S.; Yano, S. *Macromol. Symp.* **1994,** 82, (1), 173-184.

39. Shimizu, T.; Tanaka, Y.; Kutsumizu, S.; Yano, S. *Macromolecules.* **1996,** 29, (1), 156-164.

40. Guyot, B.; Boutevin, B.; Améduri, B. *Macromol. Chem. Phys.* **1996,** 197, (3), 937-952.

41. Atlas, S.; Raihane, M.; Hult, A.; Malkoch, M.; Lahcini, M.; Ameduri, B. *J. Polym. Sci., Part A: Polym. Chem.* **2013,** 51, (18), 3856-3866.

42. Wadekar, M. N.; Patil, Y. R.; Ameduri, B. *Macromolecules.* **2013,** 47, (1), 13-25.

43. Lopez, G.; Ajellal, N.; Thenappan, A.; Ameduri, B. *J. Polym. Sci., Part A: Polym. Chem.* **2014,** 52, (12), 1714-1720.

44. Dreher, W. R.; Singh, A.; Urban, M. W. *Macromolecules.* **2005,** 38, (11), 4666-4672.

45. Borkar, S.; Sen, A.; Shallenberger, J. R. *J. Polym. Sci., Part A: Polym. Chem.* **2006,** 44, (3), 1225-1232.

46. Wang, W.; Yan, D.; Bratton, D.; Howdle, S. M.; Wang, Q.; Lecomte, P. *Adv. Mater.* **2003,** 15, (16), 1348-1352.

47. Grignard, B.; Jérôme, C.; Calberg, C.; Detrembleur, C.; Jérôme, R. *J. Polym. Sci., Part A: Polym. Chem.* **2007,** 45, (8), 1499-1506.

48. Patil, Y.; Ameduri, B. *Polym. Chem.* **2013,** 4, (9), 2783-2799.

49. Girard, E.; Liu, X.; Marty, J.-D.; Destarac, M. *Polym. Chem.* **2014,** 5, (3), 1013-1022.

50. Girard, E.; Tassaing, T.; Camy, S.; Condoret, J.-S.; Marty, J.-D.; Destarac, M. *J. Am. Chem. Soc.* **2012,** 134, (29), 11920-11923.

51. Liu, L.; Lu, D.; Wang, H.; Dong, Q.; Wang, P.; Bai, R. *Chem. Commun.* **2011,** 47, (27), 7839-7841.

52. Wang, P.; Dai, J.; Liu, L.; Dong, Q.; Jin, B.; Bai, R. *Polym. Chem.* **2013,** 4, (6), 1760-1764.

53. Wang, P.; Dai, J.; Liu, L.; Dong, Q.; Wang, H.; Bai, R. *Polym. Chem.* **2014**, DOI: 10.1039/C4PY00902A

54. Keddie, D. J.; Moad, G.; Rizzardo, E.; Thang, S. H. *Macromolecules.* **2012,** 45, (13), 5321-5342.

55. Aoyagi, N.; Endo, T. *J. Polym. Sci., Part A: Polym. Chem.* **2009,** 47, (14), 3702-3709.

56. Li, L. *MALDI Mass Spectrometry for Syntetic Polymer Analysis* **2010,** John Wiley & Sons, Inc., Hoboken, New Jersey., ISBN: 978-0-471-77579-9.

57. Fineman, M.; Ross, S. D. *Journal of Polymer Science* **1950,** 5, (2), 259-262.

58. F. Tüdos; T. Kelen; T. Folders-Bereznich; Turcsanyi, B. *Journal of Macromolecular Science: Part A - Chemistry* **1976,** 10, (8), 1513-1540.

59. Mayo, F. R.; Walling, C. *Chem. Rev.* **1950,** 46, (2), 191-287.

60. Koiry, B. P.; Klok, H.-A.; Singha, N. K. *J. Fluorine. Chem.* **2014**, DOI: 10.1016/j.jfluchem.2014.06.016.

61. Narita, T. *Prog. Polym. Sci.* **1999,** 24, (8), 1095-1148.

62. J. Brandrup, E. H. I., E. A. Grulke. *Polymer Handbook, 2 Volumes Set, 4th Edition* **2003,** JOHN WILEY&SONS, INC. Canada, ISBN: 978-0-471-47936-9.